

Reinforcement Learning Under Algorithmic Triage

Eleni Straitouri¹, Adish Singla¹, Vahid Balazadeh Meresht², Manuel Gomez Rodriguez¹

¹Max Planck Institute for Software Systems, {estraitouri, adishs, manuelgr}@mpi-sws.org

²University of Toronto, balazadehvahid@gmail.com

Abstract

Methods to learn under algorithmic triage have predominantly focused on supervised learning settings where each decision, or prediction, is independent of each other. Under algorithmic triage, a supervised learning model predicts a fraction of the instances and humans predict the remaining ones. In this work, we take a first step towards developing reinforcement learning models that are optimized to operate under algorithmic triage. To this end, we look at the problem through the framework of options and develop a two-stage actor-critic method to learn reinforcement learning models under triage. The first stage performs offline, off-policy training using human data gathered in an environment where the human has operated on their own. The second stage performs on-policy training to account for the impact that switching may have on the human policy, which may be difficult to anticipate from the above human data. Extensive simulation experiments in a synthetic car driving task show that the machine models and the triage policies trained using our two-stage method effectively complement human policies and outperform those provided by several competitive baselines.

1 Introduction

Learning under algorithmic triage is a new learning paradigm which seeks the development of machine learning models that operate under different automation levels—models that take decisions for a given fraction of instances and leave the remaining ones to humans [36, 40]. This new paradigm has also been referred to as learning under human assistance [11, 12], learning to complement humans [53, 2], and learning to defer to an expert [33]. In learning under algorithmic triage, one does not only have to find a machine learning model but also a triage policy which determines who decides, the model or the human, and when.

Existing works have shown early success at fulfilling the promise of algorithmic triage—by working together, they have shown that humans and machine learning models achieve a considerably better performance than each of them would achieve on their own. However, they have predominantly focused on supervised learning settings where each decision, or prediction, is independent of each other. A very recent notable exception is the work by Meresht et al. [32], which learns to switch control between machine and human agents in a reinforcement learning setting where decisions are dependent. However, in contrast to our work, the policies of the machine agents are (pre-)trained to operate under full automation. While their problem setting is different, a natural extension of their algorithm to our setting achieves lower performance than ours.

In this paper, our goal is to develop reinforcement learning models that are optimized to operate under algorithmic triage. Similarly as in supervised learning, one of the main challenges is that, for each potential triage policy, there is an optimal machine agent, however, the triage policy is also something one seeks to optimize. Moreover, in comparison with supervised learning, we face two additional challenges. First, due to safety concerns, the vast majority of reinforcement learning models are trained using simulator environments [13, 47, 55]. Unfortunately, in these environments, human data is typically very limited and, as a result, an accurate estimation of human policies is challenging [9, 8, 31, 43, 27]. Second, the presence of switching introduces an additional cognitive load on the sequential decision making process [4]. As a result, human policies may worsen in ways that are difficult to anticipate from historical human data.

Our approach. We first introduce a modeling framework to learn reinforcement learning models under triage, which builds upon the framework of options [45, 37, 1, 23]. In the framework of options, an option policy determines which intra-option policy picks actions until termination, as dictated by a termination policy, at which point the procedure is repeated. In our modeling framework, the machine and human policies are the intra-option policies, the triage policy is the option policy, and the termination policy does not need to be explicitly defined because options are interrupting [45], *i.e.*, whenever the current intra-option policy is no longer the best choice, termination occurs. Here, note that, in contrast with the original framework of options, one of the intra-option policies—the human policy—is fixed.

Building on the above modeling framework, we introduce a two-stage actor-critic method to train the triage policy and the machine policy. In the first stage, we perform offline, off-policy training of the machine and triage policies using human data gathered in an environment where the human has operated on their own. In the second stage, we perform on-policy training to optimize the machine and triage policies trained in the first stage. Our goal is to benefit from historical human data and guarantee safety in the first stage and to account for the impact that switching may have on the human policy in the second stage. Finally, we perform a variety of simulation experiments in a synthetic car driving task. Our results show that the machine models and triage policies trained using our two-stage method effectively complement human policies and outperform those provided by several competitive baselines.¹

Further related work. Our work is also related to the areas of learning to defer and human-machine collaboration. In learning to defer, the goal is to design classifiers that are able to defer decisions [3, 6, 14, 15, 29, 41, 49, 58]. To this end, they learn to defer either by considering the defer action as an additional label value or by training an independent classifier to decide about deferred decisions. However, there are no human experts who make predictions whenever the classifiers defer them—they just pay a constant cost every time they defer predictions. Moreover, the classifiers are trained to predict the labels of all samples in the training set as in full automation. The extensive body of work on human-machine collaboration has predominantly considered settings in which the machine and the human interact with each other [5, 16, 17, 18, 19, 25, 30, 34, 35, 39, 42, 48, 50, 51, 52, 54]. In this context, our work is more closely connected to a line of work that studies switching behavior and switching costs in the context of human-computer interaction [7, 20, 22, 24, 26], which we see as complementary. abbrvnat

2 Learning Under Triage as Learning Options

Let \mathcal{S} be the state space, \mathcal{A} be the set of actions, $c(s, a)$ be the environment cost of action a at state s , and the transition dynamics of the environment are given by $p(s' | s, a)$. Then, in reinforcement learning under triage, one needs to find:

- (i) a triage policy $\tau(d | s) : \mathcal{S} \times \{0, 1\} \rightarrow [0, 1]$, which determines who takes an action at state s denoted by $d(s)$ —the machine ($d(s) = 1$) or the human ($d(s) = 0$). In the remainder, for simplicity, we will write $\tau(d = 1 | s) = \tau(s)$.
- (ii) a machine policy $\pi_{\mathbb{M}}(a | s) : \mathcal{S} \times \mathcal{A} \rightarrow [0, 1]$, which determines which actions are taken for those states s for which $d(s) = 1$.

In the above, the human takes actions according to a policy $\pi_{\mathbb{H}}(a | s) : \mathcal{S} \times \mathcal{A} \rightarrow [0, 1]$. Here, for simplicity, we assume that the human policy satisfies the Markov property, *i.e.*, it depends only on the current state s , a common assumption in the machine learning, psychology, cognitive science and economics literature. While it is possible to convert a non-Markovian human policy into a Markovian one in certain cases just by changing the state representation [10], addressing the problem of learning under triage in a semi-Markovian setting is left as a very interesting venue for future work.

Then, similarly as in standard reinforcement learning, we look for the triage and machine policies that result into the lowest expected cost (or, the highest expected reward). To this end, we define the value

¹To facilitate research in this area, we will release an open-source implementation of our algorithms with the final version of the paper.

function and the action value function under the triage policy τ as (see Appendix for details)

$$v^\tau(s) = \bar{c}_c(\tau(s)) + \sum_{a \in \mathcal{A}} [\tau(s)\pi_{\mathbb{M}}(a|s) + (1 - \tau(s))\pi_{\mathbb{H}}(a|s)] \sum_{s' \in \mathcal{S}} p(s'|s, a) [c(s, a) + v^\tau(s')] \quad (1)$$

and

$$q^\tau(s, a) = \sum_{s' \in \mathcal{S}} p(s'|s, a) [c(s, a) + v^\tau(s')], \quad (2)$$

with $\bar{c}_c(\tau(s)) = \tau(s)c_c(1) + (1 - \tau(s))c_c(0)$, where $c_c(d)$ is the cost of giving control to the human ($d = 0$) or the machine ($d = 1$) at state s , and $c(s, a)$ is the environment cost. Note that we consider an undiscounted reward setting and assume that termination occurs surely under any policy for any initial state [38].

To design our two-stage actor-critic method, it will also be useful to look at the problem from the perspective of the options framework [45]. Under this framework, an option policy determines which intra-option policy picks actions until termination, as dictated by a termination policy, at which point the procedure is repeated. In our setting, the machine policy $\pi_{\mathbb{M}}$ and the human policy $\pi_{\mathbb{H}}$ are the intra-option policies, the triage policy τ is the option policy, and the termination policy does not need to be explicitly defined because options are considered as interrupting [45], *i.e.*, whenever the current intra-option policy is no longer the best choice, termination occurs. In this context, the choice of intra-option policies depends on the option value function

$$\begin{aligned} Q^\tau(s, 1) &= c_c(1) + \sum_{a \in \mathcal{A}} \pi_{\mathbb{M}}(a|s) q^\tau(s, a) \\ Q^\tau(s, 0) &= c_c(0) + \sum_{a \in \mathcal{A}} \pi_{\mathbb{H}}(a|s) q^\tau(s, a), \end{aligned} \quad (3)$$

which is essentially the action value function for options.

3 Overview of Two-stage Actor-Critic Method

To train the triage policy and machine policy, we introduce a two-stage actor-critic method:

- I. The first stage performs offline, off-policy training using human data gathered in an environment where the human has operated on their own. More formally, it seeks to find the triage and machine policy that minimize the mean of the value function v^τ with respect to the stationary state distribution induced by the human policy $\pi_{\mathbb{H}}$ operating on its own.
- II. The second stage performs on-policy training to optimize the machine and triage policies trained in the first stage by minimizing the mean of the value function v^τ with respect to the stationary state distribution induced by the human policy $\pi_{\mathbb{H}}$ and the machine policy $\pi_{\mathbb{M}}$ operating together, as dictated by the triage policy τ .

To this end, we will parameterize both the machine policy (the actor) and the value function (the critic), and express the triage policy in terms of the parameterized value function. In the next two sections, we provide more details of each stage in turn. All the proofs are provided in the Appendix.

4 Offline Off-policy Training Using Human Data

In this section, we first discuss the training of the parameterized machine policy under the true value function and then discuss how to approximate the true value function. Throughout the section, we build upon a recent line of work on offline off-policy training [46, 21, 56], which we adapt to our specific problem setting. Similarly as in this line of work, we assume that the behavioral policy—the human policy—satisfies the

coverage assumption and, for any initial state, termination occurs surely under the target policy—the human and machine policies operating together, as dictated by the triage policy.

Actor. Let $\mathcal{M}(\Theta)$ be a class of parameterized machine policies. Then, our goal is to find the parameters $\theta \in \Theta$ that minimize the following objective function:

$$J(\theta) = \mathbb{E}_{s \sim d_{\pi_{\mathbb{H}}}}[v^\tau(s)] = \sum_{s \in \mathcal{S}} d_{\pi_{\mathbb{H}}}(s) \left(\bar{c}_c(\tau(s)) + \sum_{a \in \mathcal{A}} [\tau(s)\pi_{\mathbb{M},\theta}(a|s) + (1 - \tau(s))\pi_{\mathbb{H}}(a|s)] q^\tau(s, a) \right), \quad (4)$$

where $d_{\pi_{\mathbb{H}}}$ denotes the stationary state distribution induced by the human policy $\pi_{\mathbb{H}}(\cdot|s)$.

To facilitate our analysis, we will initially assume that τ is fixed and independent of θ and later on relax this assumption. Under this assumption, the gradient of the above objective function is given by the following theorem:

Theorem 1. *The gradient of the function $J(\theta)$ with respect to the parameters θ is given by:*

$$\frac{\partial J}{\partial \theta} = \sum_{s \in \mathcal{S}} m(s) \sum_{a \in \mathcal{A}} \frac{\partial \pi_{\mathbb{M},\theta}}{\partial \theta} q^\tau(s, a) \quad (5)$$

where τ is a fixed triage policy independent of θ , the often called emphatic weightings $\mathbf{m} = [m(s)]_{s \in \mathcal{S}}$ are given by $\mathbf{m} = (\mathbf{I} - \mathbf{P}^T)^{-1} \mathbf{D} \mathbf{d}_{\pi_{\mathbb{H}}}$ with $\mathbf{d}_{\pi_{\mathbb{H}}} = [d_{\pi_{\mathbb{H}}}(s)]_{s \in \mathcal{S}}$, $\mathbf{D} = \text{diag}(\tau)$ is a diagonal matrix with entries based on $\tau(s)$, and $\mathbf{P} = [P(s, s')]_{s, s' \in \mathcal{S}}$ where

$$P(s, s') = \sum_{a \in \mathcal{A}} (\tau(s)\pi_{\mathbb{M},\theta}(a|s) + (1 - \tau(s))\pi_{\mathbb{H}}(a|s)) p(s'|s, a).$$

However, in practice, to apply the above theorem, we need an estimate of both the emphatic weightings and the product of the gradients of the machine action policy and the action value function from a set of recorded human trajectories $\mathcal{D} = \{\mathcal{T}\}$ with $\mathcal{T} = \{(s_t, a_t)\}$. For the former, the following proposition equips us with a sequential update rule for an emphatic weighting estimator M_t with desirable properties:

Proposition 1. *multiline Let $M_t \leftarrow d(s_t) + \varrho_t M_{t-1}$, where $\varrho_t = \frac{\varpi(a_t|s_t)}{\pi_{\mathbb{H}}(a_t|s_t)}$ and*

$$\varpi(a_t|s_t) = d(s_t)\pi_{\mathbb{M},\theta}(a_t|s_t) + (1 - d(s_t))\pi_{\mathbb{H}}(a_t|s_t).$$

Then, it holds that $m(s) = d_{\pi_{\mathbb{H}}}(s) \lim_{t \rightarrow \infty} \mathbb{E}[M_t|s_t = s]$.

For the latter, we resort to a commonly used estimator with sequential update rule $\rho_t \delta_t \nabla_\theta \ln \pi_{\mathbb{M},\theta}$, where $\delta_t = c(s_t, a_t) + v^\tau(s_{t+1}) - v^\tau(s_t)$ and $\rho_t = \frac{\pi_{\mathbb{M},\theta}(a_t|s_t)}{\pi_{\mathbb{H}}(a_t|s_t)}$. After combining both estimators, we have the following proposition:

Proposition 2. *Let M_t be given by Proposition 1, $\delta_t = c(s_t, a_t) + v^\tau(s_{t+1}) - v^\tau(s_t)$ and $\rho_t = \frac{\pi_{\mathbb{M},\theta}(a_t|s_t)}{\pi_{\mathbb{H}}(a_t|s_t)}$. Then,*

$$\lim_{t \rightarrow \infty} \mathbb{E}[M_t \rho_t \delta_t \nabla_\theta \ln \pi_{\mathbb{M},\theta}] = \sum_{s \in \mathcal{S}} m(s) \sum_{a \in \mathcal{A}} \frac{\partial \pi_{\mathbb{M},\theta}}{\partial \theta} q^\tau(s, a)$$

Consequently, the above results readily yield the following update rule for the parameters of the machine policy:

$$\theta_{t+1} \leftarrow \theta_t - \alpha_t M_t \rho_t \delta_t \nabla_\theta \ln \pi_{\mathbb{M},\theta}(a_t|s_t)|_{\theta=\theta_t} \quad (6)$$

where α_t is the learning rate.

Next, we lift the assumption on the triage policy τ and let it be an ϵ -greedy policy with respect to the option value function Q^τ :

$$\tau_\theta(s) := \begin{cases} 1 - \frac{\epsilon}{2} & \text{if } Q^\tau(s, 1) \leq Q^\tau(s, 0) \\ \frac{\epsilon}{2} & \text{otherwise} \end{cases} \quad (7)$$

While under this definition, τ depends on θ because Q^τ implicitly depends on θ , the following proposition shows that gradient of the objective function $J(\theta)$ remains unchanged.

Theorem 2. Let $\tau(s)$ be an ϵ -greedy policy with respect to Q^τ , then, $\partial J / \partial \theta$ is still given by Eq. 5.

So far, we have assumed that the human policy $\pi_{\mathbb{H}}(a|s)$ and the value function v^τ are known. However, in practice, we need to estimate their values to be able to compute ϱ_t and δ_t . To estimate the human policy, we can just use a Montecarlo estimate $\hat{\pi}_{\mathbb{H}}(a|s)$ from the recorded human trajectories \mathcal{D} , i.e., $\hat{\pi}_{\mathbb{H}}(a|s) = \sum_t \mathbb{I}(a_t = a, s_t = s) / \mathbb{I}(s_t = s)$. To estimate the value function, we will resort to a critic, which we discuss next.

Critic. We adapt the one step update proposed in the options framework [1] to our offline, off-policy setting with emphatic weightings. To this end, we start by rewriting the value function in terms of the option value function, i.e.,

$$v^\tau(s) = \tau(s)Q^\tau(s, 1) + (1 - \tau(s))Q^\tau(s, 0),$$

and approximating the option value function using a linear function, i.e., $Q_{\theta}^\tau(s, d(s)) = \theta^T \phi(s, d(s)) + c_c(d(s))$, where $\theta \in \mathbb{R}^n$ is a parameter vector and $\phi(s, d(s)) \in \mathbb{R}^n$ is a feature vector.² Then, given a set of recorded human trajectories \mathcal{D} , we use the following update rule, based on ETD(0) [46], to estimate θ :

$$\theta_{t+1} \leftarrow \theta_t + \beta_t F_t \varrho_t [C_{t+1} + Q_{\theta_t}^\tau(s_{t+1}, d(s_{t+1})) - Q_{\theta_t}^\tau(s_t, d(s_t))] \nabla Q_{\theta_t}^\tau(s_t, d(s_t)) |_{\theta=\theta_t}, \quad (8)$$

where $C_{t+1} = c(s_t, a_t) + c_c(d(s_t))$, $\varrho_t = \frac{\varpi(a_t|s_t)}{\pi_{\mathbb{H}}(a_t|s_t)}$, $F_t = i(s_t) + \varrho_{t-1}F_{t-1}$ is the emphatic weighting, with $i(s_t) \in \{0, 1\}$, and β_t is the learning rate. Here, one may think of setting $i(s_t) = 1$ for states that have been visited by the human operating on their own and $i(s_t) = 0$ otherwise and can estimate the human policy $\pi_{\mathbb{H}}$ similarly as in the actor training. Moreover, note that F_t is the counterpart of M_t in the actor training with $i(s_t)$ instead of $d(s_t)$.

Whenever τ is fixed and independent of Q^τ , we are able to prove almost sure asymptotic convergence of the above update rule. In practice, we have observed good empirical performance whenever τ is a ϵ -greedy policy with respect to Q^τ . Before we proceed with the analysis, we rewrite the second term of the right hand side of Eq. 8 as:

$$\beta_t \left[\underbrace{F_t \varrho_t (C_{t+1} + c_c(d(s_{t+1})) - c_c(d(s_t))) \phi(s_t, d(s_t))}_{\mathbf{b}_t} - \underbrace{F_t \varrho_t \phi(s_t, d(s_t)) (\phi(s_t, d(s_t)) - \phi(s_{t+1}, d(s_{t+1})))^T}_{\mathbf{A}_t} \theta_t \right]$$

Following Yu [56], if we are able to show that the following conditions are satisfied, then we can guarantee almost sure asymptotic convergence of the above update rule:

- The human policy satisfies the coverage assumption and induces an irreducible Markov chain.
- Termination occurs surely under target policy for any initial state, meaning $(I - \mathbf{P})^{-1}$ exists.
- The learning rate sequence $\{\beta_t\}$ satisfies $\beta_t \in (0, 1]$, $\sum_t \beta_t < \infty$, $\sum_t \beta_t^2 < \infty$, is deterministic and eventually non increasing.
- $\mathbf{A} = \lim_{t \rightarrow \infty} \mathbb{E}_\mu[\mathbf{A}_t]$ is non singular.

The first two conditions are satisfied by assumption, the third condition only requires to set β_t accordingly. and the fourth condition is satisfied if \mathbf{A} is positive definite, a property that we also need for the update rule to be stable [46]. To prove the latter, we first rewrite \mathbf{A} as (refer to the Appendix for details) $\mathbf{A} = \Phi^T \mathbf{F} (I - \mathbf{P}) \Phi$, where $\Phi = \mathbf{D} \Phi_1 + (I - \mathbf{D}) \Phi_0$, with Φ_d a $|S| \times n$ matrix with rows $\phi^T(s, d)$, \mathbf{P}, \mathbf{D} are defined in Theorem 1 and \mathbf{F} a diagonal matrix with elements $f(s)$. Then, it is easy to see that, to prove that \mathbf{A} is positive definite, it is sufficient to prove that $\mathbf{K} = \mathbf{F} (I - \mathbf{P})$ is positive definite. To this end, we have the following claim:

Claim 1. A symmetric matrix \mathbf{K} , with positive diagonal and negative off diagonal elements, is positive definite if each row sum plus the corresponding column sum of it is positive

²We note that the linear representation is considered for the theoretical results; in the experiments we use neural representations.

ALGORITHM 1: Actor-critic method for off-policy training

Input: Q_{ϑ}^{τ} , $\pi_{\mathbb{M},\theta}$, $\pi_{\mathbb{H}}$, c , c_c , ϵ , i , α , β , set of trajectories \mathcal{D} **Initialize:** $F_0 \leftarrow 0$, $M_0 \leftarrow 0$, $\varrho_0 \leftarrow 1$, $t \leftarrow 0$, $\theta_0 \sim \mathcal{N}(0, 1)$, $\vartheta_0 \sim \mathcal{N}(0, 1)$.**for** trajectory \mathcal{T} **in** \mathcal{D} **do**

for (s_t, a_t, s_{t+1}) **in** \mathcal{T} **do**

$t \leftarrow t + 1$
 $d_t \leftarrow \epsilon\text{-greedy}(Q_{\vartheta_t}^{\tau}(s_t, 0), Q_{\vartheta_t}^{\tau}(s_t, 1))$
// critic update
 $C_{t+1} \leftarrow c(s_t, a_t) + c_c(d_t)$
 $F_t \leftarrow i(s_t) + \varrho_{t-1}F_{t-1}$
 $\varrho_t \leftarrow \frac{d_t \pi_{\mathbb{M}}(a_t | s_t) + (1-d_t) \pi_{\mathbb{H}}(a_t | s_t)}{\pi_{\mathbb{H}}(a_t | s_t)}$
 $d_{t+1} \leftarrow \epsilon\text{-greedy}(Q_{\vartheta_t}^{\tau}(s_{t+1}, 0), Q_{\vartheta_t}^{\tau}(s_{t+1}, 1))$
 $\delta_t^Q \leftarrow C_{t+1} + Q_{\vartheta_t}^{\tau}(s_{t+1}, d_{t+1}) - Q_{\vartheta_t}^{\tau}(s_t, d_t)$
 $\vartheta_{t+1} \leftarrow \vartheta_t + \beta_t F_t \varrho_t \delta_t^Q \nabla_{\vartheta} Q_{\vartheta}^{\tau}(s_t, d_t)|_{\vartheta=\vartheta_t}$
// actor update
 $\delta_t = c(s_t, a_t) + Q_{\vartheta_t}^{\tau}(s_{t+1}, d_{t+1}) - Q_{\vartheta_t}^{\tau}(s_t, d_t)$
 $\rho_t = \frac{\pi_{\mathbb{M},\theta}(a_t | s_t)}{\pi_{\mathbb{H}}(a_t | s_t)}$
 $M_t \leftarrow d_t + \varrho_{t-1}M_{t-1}$
 $\theta_{t+1} \leftarrow \theta_t - \alpha_t M_t \rho_t \delta_t \nabla_{\theta} \ln \pi_{\mathbb{M},\theta}(a_t | s_t)|_{\theta=\theta_t}$

end

end**return** θ_t, ϑ_t

Then, we only need to compute each row sum plus the corresponding column sum of \mathbf{K} to verify if \mathbf{K} is positive definite. Since \mathbf{P} is a stochastic matrix, the row sums of \mathbf{K} will be 0, so the column sums of \mathbf{K} must be positive. Now, we can find the column sums of \mathbf{K} if we multiply it with a row vector with all elements equal to 1. So the row vector of the column sums of \mathbf{K} are given by:

$$\mathbf{1}^T \mathbf{F}(\mathbf{I} - \mathbf{P}) \stackrel{(i)}{=} \mathbf{d}_{\pi_{\mathbb{H}}}^T \mathbf{D}_i (\mathbf{I} - \mathbf{P})^{-1} (\mathbf{I} - \mathbf{P}) = \mathbf{d}_{\pi_{\mathbb{H}}}^T \mathbf{D}_i,$$

where $\mathbf{D}_i = \text{diag}(i(s))$, $\mathbf{f} = [f(s)]_{s \in \mathcal{S}}$ and, in (i), we have used that $\mathbf{f} = (\mathbf{I} - \mathbf{P}^T)^{-1} \mathbf{D}_i \boldsymbol{\mu}$. As a result, it readily follows that, if $i(s) = 1$ for all $s \in \mathcal{S}$, then \mathbf{K} is positive definite. Even if that is not the case, if $i(s) \geq 0$ and there are n linearly independent feature vectors of states with $f(s) > 0$, it can be shown that \mathbf{K} is also positive definite [56].

We summarize the resulting actor-critic method for off-policy training in Algorithm 1.

5 On-policy Training Using Machine and Human Data

In this section, we proceed similarly as in the previous section. We first discuss the training of the parameterized machine policy under the true value function and then the approximation of the true value function.

Actor. Let $\mathcal{M}(\Theta)$ be a class of parameterized machine policies and, given a human policy $\pi_{\mathbb{H}}$ and machine policy $\pi_{\mathbb{M},\theta}$, denote the action policy induced by the triage policy τ as

$$\pi_{\theta}(a | s) = \tau(s) \pi_{\mathbb{M},\theta}(a | s) + (1 - \tau(s)) \pi_{\mathbb{H}}(a | s) \quad (9)$$

Then, our goal is to find the parameters $\theta \in \Theta$ that minimize the following objective function:

$$J(\theta) = \mathbb{E}_{s \sim d_{\pi_{\theta}}}[v^{\tau}(s)] = \sum_{s \in \mathcal{S}} d_{\pi_{\theta}}(s) \left(\bar{c}_c(\tau(s)) + \sum_{a \in \mathcal{A}} [\tau(s) \pi_{\mathbb{M},\theta}(a | s) + (1 - \tau(s)) \pi_{\mathbb{H}}(a | s)] q^{\tau}(s, a) \right), \quad (10)$$

where $d_{\pi_{\theta}}$ denotes the stationary state distribution induced by the policy π_{θ} .

Assume τ is fixed and independent of θ . Then, we have the following theorem, which readily follows from the standard policy gradient theorem [44]:

ALGORITHM 2: Actor-critic method for on-policy training

Input: Q_{ϑ}^{τ} , $\pi_{\mathbb{M},\theta}$, c , c_c , ϵ , α , β , #episodes.

Initialize $\theta_0 \sim \mathcal{N}(0, 1)$, $\vartheta_0 \sim \mathcal{N}(0, 1)$, $t \leftarrow 0$

for $j \in 1, 2, \dots, \text{\#episodes}$ **do**

while *episode is not terminated* **do**

$t \leftarrow t + 1$

$d_t \leftarrow \epsilon\text{-greedy}(Q_{\vartheta_t}^{\tau}(s_t, 0), Q_{\vartheta_t}^{\tau}(s_t, 1))$

 Sample a_t based on d_t and s_t ; get next state s_{t+1}

 // critic update

$C_{t+1} \leftarrow c(s_t, a_t) + c_c(d_t)$

$d_{t+1} \leftarrow \epsilon\text{-greedy}(Q_{\vartheta_t}^{\tau}(s_{t+1}, 0), Q_{\vartheta_t}^{\tau}(s_{t+1}, 1))$

$\delta_t^Q \leftarrow C_{t+1} + Q_{\vartheta_t}^{\tau}(s_{t+1}, d_{t+1}) - Q_{\vartheta_t}^{\tau}(s_t, d_t)$

$\vartheta_{t+1} \leftarrow \vartheta_t + \beta_t \delta_t^Q \nabla_{\vartheta} Q_{\vartheta}^{\tau}(s_t, d_t)|_{\vartheta=\vartheta_t}$

 // actor update

$v_{\vartheta_t}^{\tau} \leftarrow d_t Q_{\vartheta_t}^{\tau}(s_t, 1) + (1 - d_t) Q_{\vartheta_t}^{\tau}(s_t, 0)$

$\theta_{t+1} \leftarrow \theta_t - \alpha_t d_t v_{\vartheta_t}^{\tau} \nabla_{\theta} \ln \pi_{\mathbb{M},\theta}(a_t | s_t)|_{\theta=\theta_t}$

end

end

return θ_t, ϑ_t

Theorem 3. *The gradient of the function $J(\theta)$ with respect to the parameters θ is given by:*

$$\frac{\partial J}{\partial \theta} = \mathbb{E}_{s \sim d_{\pi_{\theta}}} \left[\tau(s) v^{\tau}(s) \frac{\nabla_{\theta} \pi_{\mathbb{M},\theta}(a | s)}{\pi_{\mathbb{M},\theta}(a | s)} \right] \quad (11)$$

The above result yields the following update rule for the parameters of the machine policy:

$$\theta_{t+1} \leftarrow \theta_t - \alpha_t d(s_t) v^{\tau}(s_t) \frac{\nabla_{\theta} \pi_{\mathbb{M},\theta}(a_t | s_t)|_{\theta=\theta_t}}{\pi_{\mathbb{M},\theta}(a_t | s_t)}, \quad (12)$$

where α_t is the learning rate. Here, note that the parameters of the machine policy are only updated whenever the triage policy let the machine take action ($d(s_t) = 1$). Moreover, if α_t is chosen properly, one can use standard arguments to show that the above update rule converges.

Now, assume the triage policy τ is chosen ϵ -greedily with respect to the option value function, *i.e.*, τ is given by Eq. 7. Then, it can be shown similarly as in the previous section that the gradient of v^{τ} remains the same and thus Theorem 3 still holds and we can still use the update rule given by Eq. 12 to find the parameters of the machine policy.

In the above, we have assumed that the value function v^{τ} is known. However, in practice, we will estimate their value using a critic, which we discuss next.

Critic. Here, we use the same linear approximation for the option value function as in the previous section, *i.e.*, $\hat{Q}^{\tau}(s, d(s)) = \vartheta^T \phi(s, d(s)) + c_c(d(s))$ (also, see Footnote 2). Then, we use the following update rule, based on TD(0) [44], to estimate the parameters ϑ , *i.e.*,

$$\vartheta_{t+1} \leftarrow \vartheta_t - \beta_t [C_{t+1} + Q_{\vartheta_t}^{\tau}(s_{t+1}, d(s_{t+1})) - Q_{\vartheta_t}^{\tau}(s_t, d(s_t))] \nabla_{\vartheta} Q_{\vartheta}^{\tau}(s_t, d(s_t))|_{\vartheta=\vartheta_t},$$

which can be shown to converge using standard arguments whenever τ is fixed and independent of Q .

We summarize the resulting actor-critic method for on-policy training in Algorithm 2.

6 Experiments

The goal of our experiments is to demonstrate that our two-stage actor-critic method is able to identify the limitations and complementary strengths of a given human policy and a machine policy from a given parameterized class of models. To this end, we focus on three research questions (*RQs*):

- *RQ1*: Within a given parameterized class, can our method find a machine model that when operating under triage achieves better performance than the human policy or a machine policy trained to operate on its own?
- *RQ2*: In scenarios where humans wish to keep agency, can our method find triage policies that *only* give control to the machine policy to avoid perilous situations?
- *RQ3*: In scenarios where the human policy changes due to switching, how much competitive advantage does our two-stage training process bring by adapting to these changes?

6.1 Environment for synthetic car driving task

We consider a synthetic driving task and a environment based on previous work [28, 25, 32].

Environment design, episodes, and objective. Based on the environment used in [32], we begin by generating a grid-based task, consisting of three lanes with infinite rows. Each row r is characterized by a traffic level $\gamma_r \in \{\text{no-car}, \text{light}, \text{heavy}\}$, based on which, the cell types of $r \in \{\text{road}, \text{grass}, \text{stone}, \text{car}\}$ are sampled independently at random. Refer to the Appendix for more details on the sampling of traffic levels and cell types. To train the policies, we consider an episodic setting in which, at the beginning of every episode, the driving agent starts interacting with the environment from the middle lane of a randomly chosen row and terminates after a finite horizon of 20 steps.³ The overall objective of an agent is to minimize the cost of the trajectory induced by the sequence of the actions taken during each episode.

State space. As a state representation we consider the current cell type (i.e., the type of the cell in which the agent is at the current time step), followed by the cell types of the next six rows in front. For the state feature vector representation, we use one-hot encoding of four bits (one bit for each distinct cell type), so the resulting state feature vector is of size $4 \times (1 + 6 \times 3)$, i.e., 76 bits. Once there are less than six rows in the horizon, zero-padding is used. As an agent has to learn a generalized policy that takes actions for any input state, we do not consider tabular representations and instead use neural policies for the agents as discussed below.

Action space. We assume that the chosen driving agent—which is the only one in motion—moves always forward at each time step t and decides whether to go left, straight or right, taking one of the actions in $\mathcal{A} = \{\text{left}, \text{middle}, \text{right}\}$ respectively. If the agent is either in the leftmost or rightmost lane, it will never choose an action that leads out of the grid, i.e., never chooses **left** (**right**) when in leftmost (rightmost) lane.

Cost functions. To define the environment cost $c(s, a)$, we first associate a fixed cost related to each cell type indicating its negative impact on the driving agent. We set these cell type costs as follows: **grass** as 2, **stone** as 4, **car** as 10, and **road** as 0. Given a state action pair (s, a) , we define the environment cost $c(s, a)$ as the cell type cost associated with the next cell when an action a is taken from s . For the control cost c_c , we vary it across different evaluation scenarios.

6.2 Methods and scenarios

We evaluate a total of five different methods (HUMAN, TRIAGE, MACHINE, FIXSWITCH, OPT). These methods are evaluated in three distinct scenarios (*I*, *II*, *III*), one for each *RQ*. Method OPT represents an optimal planning given a specific episode, providing an upper bound on the performance. Below, we describe the remaining methods and scenarios. We have provided the code and further implementation details as part of the supplementary material, including the neural network architectures used for the actor and the critic in different methods.⁴

Method HUMAN. This method corresponds to the human agent acting alone. In our implementation, we assume a myopic human policy which chooses an action that minimizes the one-step environment cost (with

³The presence of the agent in a cell of type **car** does not indicate episode termination, it just symbolizes proximity to another car, enough to be in danger, but not an accident.

⁴We ran all experiments on a Debian machine equipped with Intel® Xeon® E7-8857v2 CPU @ 3.00GHz and 16GB memory.

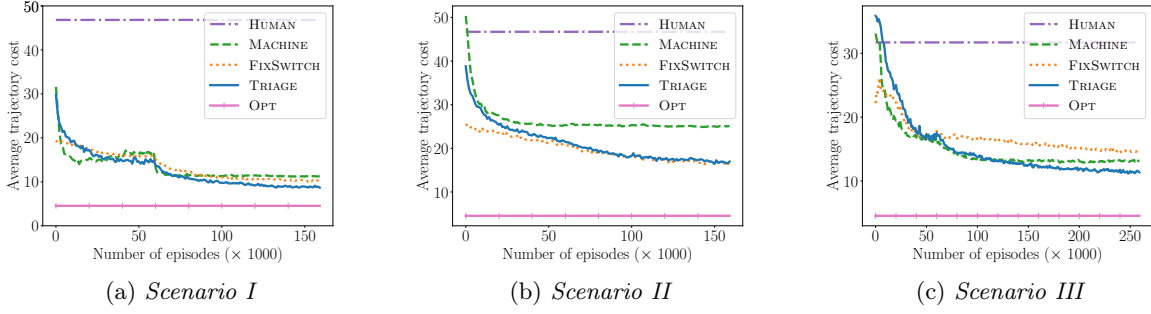


Figure 1: Test average trajectory cost against the number of training episodes. For offline training, all methods use 60K episodes. For online training, methods in *Scenario I* and *Scenario II* use 100K episodes; methods in *Scenario III* use 200K episodes. See the main text for discussion of these results.

ties being broken randomly). Apart from these myopic choices, the human policy is also suboptimal because of ignorance regarding a scenario-dependent type of obstacle that is mistakenly perceived as **road**.

Method TRIAGE. This is our two-stage actor-critic method. We consider an ϵ -greedy triage policy with respect to the option value function, that chooses between a human policy (as described in HUMAN) and a trainable machine policy (from a parametric class of models as specified per scenario). For the first offline training stage using human data, we use trajectories of the human policy operating alone for several episodes (60K) and apply Algorithm 1 for training actor and critic networks. In this stage, there is no interaction with the true environment and the training uses the recorded transitions from the human trajectories; for the computation of the emphatic weightings, we assume access to the true human policy distribution. For the second online training stage, both the actor and critic networks continue their training using Algorithm 2 while being deployed in the true environment. For the number of training episodes per stage, see Figure 1. We use the following schedule for ϵ : (a) in the first half of the offline stage we set $\epsilon = 0.2$, (b) for the second half of the offline stage we set $\epsilon = 0.1$, and (c) for the entire online stage we decay ϵ from 0.1 with rate $1/\sqrt{t}$.

Method MACHINE. This method has the same two-stage actor-critic framework as in TRIAGE, with the following crucial difference: instead of an ϵ -greedy triage policy, we assume a triage policy that always chooses the machine policy.

Method FIXSWITCH. This method also uses the same training framework as in TRIAGE, except that instead of a trainable machine policy, the ϵ -greedy triage policy chooses between the human policy and a pretrained fixed machine policy. This pretrained machine policy (*i.e.*, a fixed actor) corresponds to the machine policy at the end of the offline training stage in MACHINE.

Scenarios. We design the following three scenarios, one for each RQ , to systematically evaluate different methods:

- *Scenario I* exemplifies a situation where the performance of the human and the machine is suboptimal when operating alone: the human policy ignores cells of type **car** and any machine policy in the class ignores cells of type **grass**. We set $c_c(0) = c_c(1) = 0$.
- *Scenario II* exemplifies a situation where the human wishes to keep agency. To this end, we set $c_c(0) = 0$, $c_c(1) = 1$. Here, the human policy ignores cells of type **car** whereas any machine policy in the class perfectly recognizes all cell types.
- *Scenario III* exemplifies a situation where the human policy changes in the presence of switching. We consider a human policy which always ignores cells of type **grass**; furthermore, the human policy momentarily ignores **car** cell type at the time step of switching (as the human might not be attentive at this time). In this scenario, any machine policy ignores **stone**, and we set $c_c(0) = 1$, $c_c(1) = 0$.

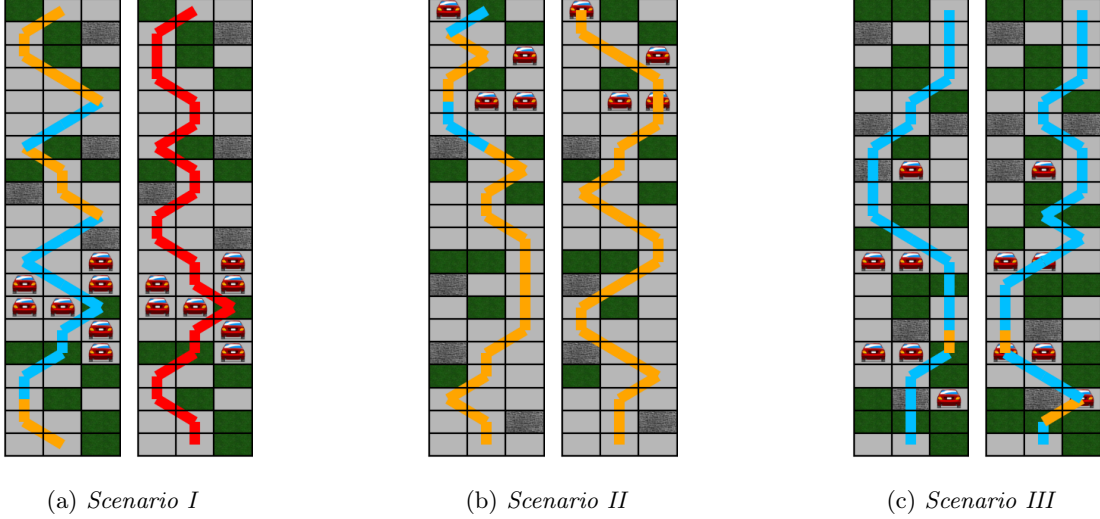


Figure 2: Illustrative trajectories for different scenarios, where orange (blue) indicates human (machine) is in control and red indicates the optimal plan. In each panel, the left trajectory always corresponds to TRIAGE and the right trajectory corresponds to (a) OPT, (b) HUMAN and (c) FIXSWITCH.

6.3 Results

In this section, we discuss results for three scenarios in the context of different *RQs*. For a quantitative comparison, we compute the average trajectory cost for the methods on a separate test set that corresponds to 1000 randomly generated episodes (each with horizon of 20 steps). Figure 1 summarizes the results for different number of training episodes. Here, for evaluation in the offline stage, we set $\epsilon = 0$ when computing the performance on the test set; in the online stage, we use the same ϵ as the one used in the corresponding training episode. For a qualitative comparison, we provide illustrative examples of trajectories induced by the examined methods at the end of the training in Figure 2.

Results for *Scenario I (RQ1)*. Recall that for the *Scenario I*, the human policy is suboptimal because it chooses actions myopically and ignores **car** cell types, and any machine policy in the considered parametric class is suboptimal because it ignores **grass** cell types. Figure 1a shows that our method TRIAGE achieves better performance than HUMAN or MACHINE. Moreover, Figure 2a highlights how our method TRIAGE is able to identify the limitations and complementary strengths of the human and the machine agent, and selectively gives control to each of them.

Results for *Scenario II (RQ2)*. Recall that for the *Scenario II*, the human agent wishes to keep agency and this is captured by control costs $c_c(0) = 0$, $c_c(1) = 1$. Similar to *Scenario I*, Figure 1b shows that TRIAGE achieves a higher performance than both HUMAN and MACHINE. Moreover, for this scenario, TRIAGE is able to find triage policies that only give control to the machine policy to avoid perilous situations (see Figure 2b for an illustrative example). Quantitatively, we note that the TRIAGE method gives about only 25% of control to the machine policy per episode in *Scenario II*, in comparison to about 45% in *Scenario I*.

Results for *Scenario III (RQ3)*. Recall that for the *Scenario III*, there is a change in human behavior in the presence of switching. As a result, while in the previous two scenarios, the FIXSWITCH method and the TRIAGE method perform comparably, in this scenario, TRIAGE exhibits a competitive advantage w.r.t. FIXSWITCH, as shown in Figure 1c. This is because the FIXSWITCH method uses a pretrained machine policy (a fixed actor) and therefore is unable to adapt to changes in the human policy, in contrast with the TRIAGE method. Figure 2c (2nd row) exemplifies the adaptation of the TRIAGE method, in contrast to that of FIXSWITCH. Here, FIXSWITCH gives control to the human as the machine policy ignores **stone** (see 3rd row, middle lane); however, this leads to an undesirable outcome as the human policy would ignore **car** momentarily

after switching (see 3rd row, right lane). As can be seen, the TRIAGE method has adapted to these changes and keeps the control with the machine policy in the 2nd row. The results in *Scenario III* highlight the importance of the second stage in our method, which enables an adaptation to unforeseen behavioral changes of the human.

7 Conclusions

In this paper, we have initiated the development of reinforcement learning models that are optimized to operate under algorithmic triage. We have formalized the problem building upon the framework of options and introduced a two-stage actor-critic method to train both the triage policy and the policy of the reinforcement learning agent. Our work opens many interesting venues for future work. For example, it would be interesting to derive convergence guarantees for the update rule used in the critic both during offline off-policy training and on-policy training whenever the triage policy depends on the option value function. In that context, an analysis of convergence for the whole actor-critic algorithm would be a breakthrough result. Moreover, in our theoretical results, we have assumed that the estimation of the human policy is perfect, however, it would be interesting to account for error estimations in the analysis. Finally, it would be valuable to assess the performance of reinforcement learning models that are optimized to operate under algorithmic triage using interventional experiments on a real-world application.

References

- [1] Pierre-Luc Bacon, Jean Harb, and Doina Precup. The option-critic architecture. In *AAAI*, 2017.
- [2] Gagan Bansal, Besmira Nushi, Ece Kamar, Eric Horvitz, and Daniel S. Weld. Optimizing AI for Teamwork. In *AAAI*, 2021.
- [3] P. Bartlett and M. Wegkamp. Classification with a reject option using a hinge loss. *JMLR*, 2008.
- [4] K. Brookhuis, D. De Waard, and W. Janssen. Behavioural impacts of advanced driver assistance systems—an overview. *European Journal of Transport and Infrastructure Research*, 1(3), 2001.
- [5] Daniel S Brown and Scott Niekum. Machine teaching for inverse reinforcement learning: Algorithms and applications. In *AAAI*, 2019.
- [6] C. Cortes, G. DeSalvo, and M. Mohri. Learning with rejection. In *ALT*, 2016.
- [7] Mary Czerwinski, Edward Cutrell, and Eric Horvitz. Instant messaging and interruption: Influence of task type on performance. In *OZCHI*, 2000.
- [8] Allan Dafoe, Edward Hughes, Yoram Bachrach, Tantum Collins, Kevin R McKee, Joel Z Leibo, Kate Larson, and Thore Graepel. Open problems in cooperative ai. *arXiv preprint arXiv:2012.08630*, 2020.
- [9] Allan Dafoe, Yoram Bachrach, Gillian Hadfield, Eric Horvitz, Kate Larson, and Thore Graepel. Cooperative ai: machines must learn to find common ground. *Nature*, 593:33–36, 2021.
- [10] Nathaniel D Daw and Peter Dayan. The algorithmic anatomy of model-based evaluation. *Philosophical Transactions of the Royal Society B: Biological Sciences*, 369(1655):20130478, 2014.
- [11] A. De, P. Koley, N. Ganguly, and M. Gomez-Rodriguez. Regression under human assistance. In *AAAI*, 2020.
- [12] Abir De, Nastaran Okati, Ali Zarezade, and Manuel Gomez-Rodriguez. Classification under human assistance. In *AAAI*, 2021.
- [13] A. Dosovitskiy, G. Ros, F. Codevilla, A. Lopez, and V. Koltun. Carla: An open urban driving simulator. *arXiv preprint arXiv:1711.03938*, 2017.

- [14] Y. Geifman and R. El-Yaniv. Selectivenet: A deep neural network with an integrated reject option. *arXiv preprint arXiv:1901.09192*, 2019.
- [15] Y. Geifman, G. Uziel, and R. El-Yaniv. Bias-reduced uncertainty estimation for deep neural classifiers. In *ICLR*, 2018.
- [16] A. Ghosh, S. Tschiatschek, H. Mahdavi, and A. Singla. Towards deployment of robust cooperative ai agents: An algorithmic framework for learning adaptive policies. In *AAMAS*, 2020.
- [17] A. Grover, M. Al-Shedivat, J. Gupta, Y. Burda, and H. Edwards. Learning policy representations in multiagent systems. In *ICML*, 2018.
- [18] D. Hadfield-Menell, S. Russell, P. Abbeel, and A. Dragan. Cooperative inverse reinforcement learning. In *NIPS*, 2016.
- [19] L. Haug, S. Tschiatschek, and A. Singla. Teaching inverse reinforcement learners via features and demonstrations. In *NeurIPS*, 2018.
- [20] Eric Horvitz and Johnson Apacible. Learning and reasoning about interruption. In *Proceedings of the 5th international conference on Multimodal interfaces*, pages 20–27, 2003.
- [21] Ehsan Imani, Eric Graves, and Martha White. An off-policy policy gradient theorem using emphatic weightings, 2019.
- [22] Shamsi T Iqbal and Brian P Bailey. Understanding and developing models for detecting and differentiating breakpoints during interactive tasks. In *CHI*, 2007.
- [23] Arushi Jain, Khimya Khetarpal, and Doina Precup. Safe option-critic: Learning safety in the option-critic architecture. *The Knowledge Engineering Review*, 36, 2021.
- [24] Christian P Janssen, Shamsi T Iqbal, Andrew L Kun, and Stella F Donker. Interrupted by my car? implications of interruption and interleaving research for automated vehicles. *International Journal of Human-Computer Studies*, 130:221–233, 2019.
- [25] Parameswaran Kamalaruban, Rati Devidze, Volkan Cevher, and Adish Singla. Interactive teaching algorithms for inverse reinforcement learning. In *IJCAI*, 2019.
- [26] Kyle Kotowick and Julie Shah. Modality switching for mitigation of sensory adaptation and habituation in personal navigation systems. In *23rd International Conference on Intelligent User Interfaces*, pages 115–127, 2018.
- [27] Vitaly Kurin, Sebastian Nowozin, Katja Hofmann, Lucas Beyer, and Bastian Leibe. The atari grand challenge dataset. *arXiv preprint arXiv:1705.10998*, 2017.
- [28] Sergey Levine, Zoran Popovic, and Vladlen Koltun. Feature construction for inverse reinforcement learning. In *NIPS*, volume 23, page 1342, 2010.
- [29] Z. Liu, Z. Wang, P. Liang, R. Salakhutdinov, L. Morency, and M. Ueda. Deep gamblers: Learning to abstain with portfolio theory. In *NeurIPS*, 2019.
- [30] O. Macindoe, L. Kaelbling, and T. Lozano-Pérez. Pomcop: Belief space planning for sidekicks in cooperative games. In *AIIDE*, 2012.
- [31] Reid McIlroy-Young, Siddhartha Sen, Jon Kleinberg, and Ashton Anderson. Aligning superhuman ai with human behavior: Chess as a model system. In *KDD*, 2020.
- [32] Vahid Balazadeh Meresht, Abir De, Adish Singla, and Manuel Gomez-Rodriguez. Learning to switch between machines and humans. *arXiv preprint arXiv:2002.04258*, 2021.

- [33] Hussein Mozannar and David Sontag. Consistent estimators for learning to defer to an expert. In *ICML*, 2020.
- [34] S. Nikolaidis, R. Ramakrishnan, K. Gu, and J. Shah. Efficient model learning from joint-action demonstrations for human-robot collaborative tasks. In *HRI*, 2015.
- [35] S. Nikolaidis, J. Forlizzi, D. Hsu, J. Shah, and S. Srinivasa. Mathematical models of adaptation in human-robot collaboration. *arXiv preprint arXiv:1707.02586*, 2017.
- [36] Nastaran Okati, Abir De, and Manuel Gomez-Rodriguez. Differentiable learning under triage. *arXiv preprint arXiv:2103.08902*, 2021.
- [37] Doina Precup and Richard S. Sutton. *Temporal Abstraction in Reinforcement Learning*. PhD thesis, University of Massachusetts Amherst, 2000. AAI9978540.
- [38] Martin L. Puterman. *Markov Decision Processes: Discrete Stochastic Dynamic Programming*. John Wiley & Sons, Inc., 1st edition, 1994.
- [39] Goran Radanovic, Rati Devidze, David C. Parkes, and Adish Singla. Learning to collaborate in markov decision processes. In *ICML*, 2019.
- [40] M. Raghu, K. Blumer, G. Corrado, J. Kleinberg, Z. Obermeyer, and S. Mullainathan. The algorithmic automation problem: Prediction, triage, and human effort. *arXiv preprint arXiv:1903.12220*, 2019.
- [41] H. Ramaswamy, A. Tewari, and S. Agarwal. Consistent algorithms for multiclass classification with an abstain option. *Electronic J. of Statistics*, 2018.
- [42] Siddharth Reddy, Anca D Dragan, and Sergey Levine. Shared autonomy via deep reinforcement learning. *arXiv preprint arXiv:1802.01744*, 2018.
- [43] James Scott, Richard Gass, Jon Crowcroft, Pan Hui, Christophe Diot, and Augustin Chaintreau. Crawdad dataset cambridge/haggle (v. 2006-09-15). *CRAWDAD wireless network data archive*, 2006.
- [44] Richard S Sutton and Andrew G Barto. *Reinforcement learning: An introduction*. MIT press, 2018.
- [45] Richard S. Sutton, Doina Precup, and Satinder Singh. Between mdps and semi-mdps: A framework for temporal abstraction in reinforcement learning. *Artificial Intelligence*, 112(1):181–211, 1999. ISSN 0004-3702. doi: [https://doi.org/10.1016/S0004-3702\(99\)00052-1](https://doi.org/10.1016/S0004-3702(99)00052-1). URL <https://www.sciencedirect.com/science/article/pii/S0004370299000521>.
- [46] Richard S. Sutton, A. Rupam Mahmood, and Martha White. An emphatic approach to the problem of off-policy temporal-difference learning. *JMLR*, 2016.
- [47] V. Talpaert et al. Exploring applications of deep reinforcement learning for real-world autonomous driving systems. *arXiv preprint arXiv:1901.01536*, 2019.
- [48] Matthew E Taylor, Halit Bener Suay, and Sonia Chernova. Integrating reinforcement learning with human demonstrations of varying ability. In *AAMAS*, 2011.
- [49] S. Thulasidasan, T. Bhattacharya, J. Bilmes, G. Chennupati, and J. Mohd-Yusof. Combating label noise in deep learning using abstention. *arXiv preprint arXiv:1905.10964*, 2019.
- [50] Lisa Torrey and Matthew Taylor. Teaching on a budget: Agents advising agents in reinforcement learning. In *AAMAS*, 2013.
- [51] S. Tschitschek, A. Ghosh, L. Haug, R. Devidze, and A. Singla. Learner-aware teaching: Inverse reinforcement learning with preferences and constraints. In *NeurIPS*, 2019.

- [52] Thomas J Walsh, Daniel K Hewlett, and Clayton T Morrison. Blending autonomous exploration and apprenticeship learning. In *NIPS*, 2011.
- [53] Bryan Wilder, Eric Horvitz, and Ece Kamar. Learning to complement humans. In *IJCAI*, 2020.
- [54] H. Wilson and P. Daugherty. Collaborative intelligence: humans and ai are joining forces. *Harvard Business Review*, 2018.
- [55] B. Wymann, E. Espié, C. Guionneau, C. Dimitrakakis, R. Coulom, and A. Sumner. Torcs, the open racing car simulator. *Software available at <http://torcs.sourceforge.net>*, 4(6), 2000.
- [56] H. Yu. On convergence of emphatic temporal-difference learning. In *COLT*, 2015.
- [57] Shangdong Zhang, Bo Liu, Hengshuai Yao, and Shimon Whiteson. Provably convergent two-timescale off-policy actor-critic with function approximation. In *ICML*, 2020.
- [58] Liu Ziyin, Blair Chen, Ru Wang, Paul Pu Liang, Ruslan Salakhutdinov, Louis-Philippe Morency, and Masahito Ueda. Learning not to learn in the presence of noisy labels. *arXiv preprint [arXiv:2002.06541](https://arxiv.org/abs/2002.06541)*, 2020.

A Derivation of Bellman's equations

Let $C_{t+1} = c_c(d(s_t)) + c(s_t, a_t)$ be the total cost at time step t and assume that the terminal states are absorbing, *i.e.*, the only transition in those states are to themselves with zero cost. Then, the value function given the switching policy τ is given by:

$$\begin{aligned} v^\tau(s) &= \mathbb{E} \left[\sum_{k=0}^{\infty} C_{t+k+1} \mid s_t=s \right] = \mathbb{E} \left[c_c(d(s_t)) + c(s_t, a_t) + \sum_{k=0}^{\infty} C_{t+k+2} \mid s_t=s \right] \\ &= \bar{c}_c(\tau(s)) + \sum_{a \in \mathcal{A}} (\tau(s) \cdot \pi_{\mathbb{M}}(a \mid s) + (1 - \tau(s))\pi_{\mathbb{H}}(a \mid s)) \\ &\quad \times \sum_{s' \in \mathcal{S}} p(s' \mid s, a) \left[c(s, a) + \mathbb{E}_\tau \left[\sum_{k=0}^{\infty} C_{t+k+2} \mid s_{t+1}=s' \right] \right] \\ &= \bar{c}_c(\tau(s)) + \sum_{a \in \mathcal{A}} (\tau(s) \cdot \pi_{\mathbb{M}}(a \mid s) + (1 - \tau(s))\pi_{\mathbb{H}}(a \mid s)) \sum_{s' \in \mathcal{S}} p(s' \mid s, a) [c(s, a) + v^\tau(s')] \end{aligned}$$

Moreover, the action value function given the switching policy τ is given by:

$$\begin{aligned} q^\tau(s, a) &= \mathbb{E}_\tau \left[\sum_{k=0}^{\infty} C_{t+k+1} \mid s_t=s, a_t=a \right] = \mathbb{E}_\tau \left[c(s_t, a_t) + \sum_{k=0}^{\infty} C_{t+k+2} \mid s_t=s, a_t=a \right] \\ &= \sum_{s' \in \mathcal{S}} p(s' \mid s, a) \left[c(s, a) + \mathbb{E}_\pi \left[\sum_{k=0}^{\infty} C_{t+k+2} \mid s_{t+1}=s' \right] \right] = \sum_{s' \in \mathcal{S}} p(s' \mid s, a) [c(s, a) + v^\tau(s')] \end{aligned}$$

B Proof of Theorem 1

By definition, we have that:

$$\frac{\partial J}{\partial \theta} = \sum_{s \in \mathcal{S}} d_{\pi_{\mathbb{H}}}(s) \frac{\partial v^\tau(s)}{\partial \theta} \quad (13)$$

Now, to compute the gradient of the value function $v^\tau(s)$, we apply the chain rule:

$$\frac{\partial v^\tau(s)}{\partial \theta} = \tau(s) \sum_{a \in \mathcal{A}} \frac{\partial \pi_{\mathbb{M}, \theta}}{\partial \theta} q^\tau(s, a) + \sum_{a \in \mathcal{A}} (\tau(s) \pi_{\mathbb{M}, \theta}(a \mid s) + (1 - \tau(s)) \pi_{\mathbb{H}}(a \mid s)) \sum_{s' \in \mathcal{S}} p(s' \mid s, a) \frac{\partial v^\tau(s')}{\partial \theta} \quad (14)$$

Next, let $\mathbf{d}_{\pi_{\mathbb{H}}} = [d_{\pi_{\mathbb{H}}}(s)]_{s \in \mathcal{S}}$, $\dot{\mathbf{v}}^\tau = \left[\frac{\partial v^\tau(s)}{\partial \theta_{s'}} \right]_{s, s' \in \mathcal{S}}$, $\mathbf{G} = [G(s, s')]_{s, s' \in \mathcal{S}}$ with

$$G(s, s') = \sum_{a \in \mathcal{A}} \frac{\partial \pi_{\mathbb{M}, \theta}(a \mid s)}{\partial \theta_{s'}} q^\tau(s, a),$$

$\mathbf{P} = [P(s, s')]_{s, s' \in \mathcal{S}}$ with

$$P(s, s') = \sum_{a \in \mathcal{A}} (\tau(s) \pi_{\mathbb{M}, \theta}(a \mid s) + (1 - \tau(s)) \pi_{\mathbb{H}}(a \mid s)) p(s' \mid s, a),$$

and $\mathbf{D} = \text{diag}(\tau)$. Then, we can rewrite Eq. 14 as:

$$\dot{\mathbf{v}}^\tau = \mathbf{D}\mathbf{G} + \mathbf{P}\dot{\mathbf{v}}^\tau \Rightarrow \dot{\mathbf{v}}^\tau = (\mathbf{I} - \mathbf{P})^{-1} \mathbf{D}\mathbf{G}$$

Therefore, we have that:

$$\frac{\partial J}{\partial \theta} = \mathbf{d}_{\pi_{\mathbb{H}}}^T \dot{\mathbf{v}}^\tau = \mathbf{d}_{\pi_{\mathbb{H}}}^T (\mathbf{I} - \mathbf{P})^{-1} \mathbf{D}\mathbf{G} = \mathbf{m}^T \mathbf{G} = \sum_{s \in \mathcal{S}} m(s) \sum_{a \in \mathcal{A}} \frac{\partial \pi_{\mathbb{M}, \theta}}{\partial \theta} q^\tau(s, a)$$

C Proof of Proposition 1

Let $\bar{m}(s) := d_{\pi_{\mathbb{H}}}(s) \lim_{t \rightarrow \infty} \mathbb{E}[M_t | s_t = s]$. Then, we have that:

$$\begin{aligned}
\bar{m}(s) &= d_{\pi_{\mathbb{H}}}(s) \lim_{t \rightarrow \infty} \mathbb{E}[d(s_t) + \varrho_{t-1} M_{t-1} | s_t = s] \\
&\stackrel{(i)}{=} d_{\pi_{\mathbb{H}}}(s) \tau(s) + d_{\pi_{\mathbb{H}}}(s) \lim_{t \rightarrow \infty} \sum_{s', a'} \mathbb{P}\{s_{t-1} = s', a_{t-1} = a' | s_t = s\} \frac{\varpi(a' | s')}{\pi_{\mathbb{H}}(a' | s')} \mathbb{E}[M_{t-1} | s_{t-1} = s'] \\
&\stackrel{(ii)}{=} d_{\pi_{\mathbb{H}}}(s) \tau(s) + d_{\pi_{\mathbb{H}}}(s) \sum_{s', a'} \frac{d_{\pi_{\mathbb{H}}}(s') \pi_{\mathbb{H}}(a' | s') p(s | s', a')}{d_{\pi_{\mathbb{H}}}(s)} \frac{\varpi(a' | s')}{\pi_{\mathbb{H}}(a' | s')} \lim_{t \rightarrow \infty} \mathbb{E}[M_{t-1} | s_{t-1} = s'] \\
&= d_{\pi_{\mathbb{H}}}(s) \tau(s) + \sum_{s'} \sum_{a'} \varpi(a' | s') p(s | s', a') d_{\pi_{\mathbb{H}}}(s') \lim_{t \rightarrow \infty} \mathbb{E}[M_{t-1} | s_{t-1} = s'] \\
&= d_{\pi_{\mathbb{H}}}(s) \tau(s) + \sum_{s'} P(s', s) \bar{m}(s'),
\end{aligned}$$

where, in (i), we have used that $\tau(s) = \lim_{t \rightarrow \infty} \mathbb{E}[d(s_t) | s_t = s]$ since $\tau(s)$ is fixed and, in (ii), we have used the Bayes rule. Now, let $\bar{\mathbf{m}} = [\bar{m}(s)]_{s \in \mathcal{S}}$. Then, we can rewrite the above expression as:

$$\bar{\mathbf{m}} = D \mathbf{d}_{\pi_{\mathbb{H}}} + P^T \bar{\mathbf{m}} \quad \Rightarrow \quad \bar{\mathbf{m}} = (I - P^T)^{-1} D \mathbf{d}_{\pi_{\mathbb{H}}}$$

Therefore, by definition, it readily follows that $\bar{\mathbf{m}} = [m(s)]_{s \in \mathcal{S}}$.

D Proof of Proposition 2

It readily follows that:

$$\begin{aligned}
\mathbb{E}[M_t \rho_t \delta_t \nabla_{\theta} \ln \pi_{\mathbb{M}, \theta}] &= \sum_s d_{\pi_{\mathbb{H}}}(s) \mathbb{E}[M_t | s_t = s] \mathbb{E}[\rho_t \delta_t \nabla_{\theta} \ln \pi_{\mathbb{M}, \theta} | s_t = s] \\
&= \sum_s m(s) \sum_a \pi_{\mathbb{H}}(a | s) \frac{\pi_{\mathbb{M}, \theta}(a | s)}{\pi_{\mathbb{H}}(a | s)} \frac{1}{\pi_{\mathbb{M}, \theta}(a | s)} \\
&\quad \times \frac{\partial \pi_{\mathbb{M}, \theta}(a | s)}{\partial \theta} \left(c(s, a) + \sum_{s'} p(s' | s, a) v^{\tau}(s') - v^{\tau}(s) \right) \\
&\stackrel{(i)}{=} \sum_s m(s) \sum_a \frac{\partial \pi_{\mathbb{M}, \theta}(a | s)}{\partial \theta} \left(\sum_{s'} p(s' | s, a) (c(s, a) + v^{\tau}(s')) - v^{\tau}(s) \right) \\
&\stackrel{(ii)}{=} \sum_s m(s) \sum_a \frac{\partial \pi_{\mathbb{M}, \theta}(a | s)}{\partial \theta} (q^{\tau}(s, a) - v^{\tau}(s)) \\
&= \sum_s m(s) \left(\sum_a \frac{\partial \pi_{\mathbb{M}, \theta}(a | s)}{\partial \theta} q^{\tau}(s, a) - v^{\tau}(s) \frac{\partial \sum_a \pi_{\mathbb{M}, \theta}(a, s)}{\partial \theta} \right) \\
&= \sum_s m(s) \left(\sum_a \frac{\partial \pi_{\mathbb{M}, \theta}(a | s)}{\partial \theta} q^{\tau}(s, a) - v^{\tau}(s) \frac{\partial 1}{\partial \theta} \right) \\
&= \sum_s m(s) \sum_a \frac{\partial \pi_{\mathbb{M}, \theta}(a | s)}{\partial \theta} q^{\tau}(s, a),
\end{aligned}$$

where, in (i), we have used $1 \cdot c(s, a) = \sum_{s'} p(s' | s, a) c(s, a)$ and, in (ii), we have used Eq. 2.

E Proof of Theorem 2

We start by explicitly writing $\tau(s) = \tau_\theta(s)$ and $Q^\tau(s, d(s)) = Q_\theta^\tau(s, d(s))$ to highlight the dependence with respect to the machine parameters θ . Moreover, under an ϵ -greedy triage policy, we have that:

$$\tau_\theta(s) = \begin{cases} 1 - \frac{\epsilon}{2} & \text{if } Q_\theta^\tau(s, 1) \leq Q_\theta^\tau(s, 0) \\ \frac{\epsilon}{2} & \text{otherwise} \end{cases} \quad (15)$$

Then, it follows that:

$$\begin{aligned} \frac{\partial v^\tau}{\partial \theta} &= \frac{\partial(\tau_\theta(s)c_c(1) + (1 - \tau_\theta(s))c_c(0))}{\partial \theta} + \sum_{a \in \mathcal{A}} \frac{\partial(\tau_\theta(s)\pi_{\mathbb{M},\theta}(a|s) + (1 - \tau_\theta(s))\pi_{\mathbb{H}}(a|s))}{\partial \theta} q^\tau(s, a) \\ &\quad + \sum_{a \in \mathcal{A}} (\tau_\theta(s)\pi_{\mathbb{M},\theta}(a|s) + (1 - \tau_\theta(s))\pi_{\mathbb{H}}(a|s)) \frac{\partial q^\tau(s, a)}{\partial \theta} \\ &= \frac{\partial \tau_\theta(s)}{\partial \theta} (c_c(1) - c_c(0)) + \sum_{a \in \mathcal{A}} \frac{\partial \tau_\theta(s)}{\partial \theta} (\pi_{\mathbb{M},\theta}(a|s) - \pi_{\mathbb{H}}(a|s)) q^\tau(s, a) \\ &\quad + \sum_{a \in \mathcal{A}} \tau_\theta(s) \frac{\partial \pi_{\mathbb{M},\theta}}{\partial \theta} q^\tau(s, a) + \sum_{a \in \mathcal{A}} (\tau_\theta(s)\pi_{\mathbb{M},\theta}(a|s) + (1 - \tau_\theta(s))\pi_{\mathbb{H}}(a|s)) \frac{\partial q^\tau(s, a)}{\partial \theta} \\ &\stackrel{(i)}{=} \frac{\partial \tau_\theta(s)}{\partial \theta} (Q_\theta^\tau(s, 1) - Q_\theta^\tau(s, 0)) + \sum_{a \in \mathcal{A}} \tau_\theta(s) \frac{\partial \pi_{\mathbb{M},\theta}}{\partial \theta} q^\tau(s, a) \\ &\quad + \sum_{a \in \mathcal{A}} (\tau_\theta(s)\pi_{\mathbb{M},\theta}(a|s) + (1 - \tau_\theta(s))\pi_{\mathbb{H}}(a|s)) \frac{\partial q^\tau(s, a)}{\partial \theta} \\ &\stackrel{(ii)}{=} \sum_{a \in \mathcal{A}} \tau_\theta(s) \frac{\partial \pi_{\mathbb{M},\theta}}{\partial \theta} q^\tau(s, a) + \sum_{a \in \mathcal{A}} (\tau_\theta(s)\pi_{\mathbb{M},\theta}(a|s) + (1 - \tau_\theta(s))\pi_{\mathbb{H}}(a|s)) \frac{\partial q^\tau(s, a)}{\partial \theta} \\ &= \sum_{a \in \mathcal{A}} \tau_\theta(s) \frac{\partial \pi_{\mathbb{M},\theta}}{\partial \theta} q^\tau(s, a) + \sum_{a \in \mathcal{A}} (\tau_\theta(s)\pi_{\mathbb{M},\theta}(a|s) + (1 - \tau_\theta(s))\pi_{\mathbb{H}}(a|s)) \sum_{s' \in \mathcal{S}} p(s'|s, a) \frac{\partial v^\tau(s')}{\partial \theta}, \end{aligned}$$

where, in (i), we have used Eq. 3 and, in (ii), we have used Lemma 1 below. Since the above expression matches Eq. 14, this concludes the proof.

Lemma 1. Let $\tau(s) = \tau_\theta(s)$ and $Q^\tau(s, d(s)) = Q_\theta^\tau(s, d(s))$. For any $s \in \mathcal{S}$ and θ , it holds that:

$$\frac{\partial \tau_\theta(s)}{\partial \theta} (Q_\theta^\tau(s, 1) - Q_\theta^\tau(s, 0)) = 0 \quad (16)$$

Proof. Let θ_0 be the point where $Q_{\theta_0}^\tau(s, 1) = Q_{\theta_0}^\tau(s, 0)$. For $\theta \neq \theta_0$, Eq. 16 holds since $\nabla_\theta \tau_\theta(s) = 0$. Now, assume that $Q_\theta^\tau(s, d(s))$ is continuous w.r.t. θ and that w.l.o.g that $Q_\theta^\tau(s, 1) > Q_{\theta_0}^\tau(s, 0)$, for $\theta = \theta_0 + \epsilon$ and $Q_\theta^\tau(s, 1) < Q_{\theta_0}^\tau(s, 0)$, for $\theta = \theta_0 - \epsilon$, for small $\epsilon > 0$. Then we have that:

$$\begin{aligned} \lim_{\theta \rightarrow \theta_0^+} \frac{\tau_\theta(s) - \tau_{\theta_0}(s)}{\theta - \theta_0} (Q_{\theta_0}^\tau(s, 1) - Q_{\theta_0}^\tau(s, 0)) &= \lim_{\theta \rightarrow \theta_0^+} \frac{\frac{\epsilon}{2} - (1 - \frac{\epsilon}{2})}{\theta - \theta_0} (Q_{\theta_0}^\tau(s, 1) - Q_{\theta_0}^\tau(s, 0)) \\ &= \lim_{\theta \rightarrow \theta_0^+} \frac{(\epsilon - 1) (Q_{\theta_0}^\tau(s, 1) - Q_{\theta_0}^\tau(s, 0))}{\theta - \theta_0} \\ &\stackrel{(i)}{=} \lim_{\theta \rightarrow \theta_0^+} \frac{(\epsilon - 1) (\nabla_\theta Q_{\theta_0}^\tau(s, 1) - \nabla_\theta Q_{\theta_0}^\tau(s, 0))}{1} \\ &= \lim_{\theta \rightarrow \theta_0^+} \frac{0}{1} = 0, \end{aligned}$$

where, in (i), we have used L'Hôpital's rule. Moreover, we also have that:

$$\begin{aligned}
\lim_{\theta \rightarrow \theta_0^-} \frac{\tau_\theta(s) - \tau_{\theta_0}(s)}{\theta - \theta_0} (Q_{\theta_0}^\tau(s, 1) - Q_{\theta_0}^\tau(s, 0)) &= \lim_{\theta \rightarrow \theta_0^-} \frac{(1 - \frac{\epsilon}{2}) - (1 - \frac{\epsilon}{2})}{\theta - \theta_0} (Q_{\theta_0}^\tau(s, 1) - Q_{\theta_0}^\tau(s, 0)) \\
&= \lim_{\theta \rightarrow \theta_0^-} \frac{((1 - \frac{\epsilon}{2}) - (1 - \frac{\epsilon}{2})) (Q_{\theta_0}^\tau(s, 1) - Q_{\theta_0}^\tau(s, 0))}{\theta - \theta_0} \\
&\stackrel{(i)}{=} \lim_{\theta \rightarrow \theta_0^-} \frac{0 \cdot (\nabla_\theta Q_{\theta_0}^\tau(s, 1) - \nabla_\theta Q_{\theta_0}^\tau(s, 0))}{1} \\
&= \lim_{\theta \rightarrow \theta_0^-} \frac{0}{1} = 0,
\end{aligned}$$

where, in (i), we have also used L'Hôpital's rule. This concludes the proof. \square

F Derivation of Matrix Equality

To show that $\mathbf{A} = \Phi^T \mathbf{F}(\mathbf{I} - \mathbf{P})\Phi$, we proceed as follows:

$$\begin{aligned}
\mathbf{A} &= \lim_{t \rightarrow \infty} \mathbb{E}[\mathbf{A}_t] = \sum_s d_{\pi_{\mathbb{H}}}(s) \mathbb{E}[F_t \varrho_t \phi(s, d_t) (\phi(s, d_t) - \phi(s, d_{t+1}))^T \mid s_t = s] \\
&= \sum_s d_{\pi_{\mathbb{H}}}(s) \mathbb{E}[F_t \mid s_t = s] \mathbb{E}[\varrho_t \phi(s, d_t) (\phi(s, d_t) - \phi(s, d_{t+1}))^T] \\
&= \sum_s f(s) \sum_a \pi_{\mathbb{H}}(a \mid s) \varrho(a, s) \mathbb{E}_{d \sim \tau(s)}[\phi(s, d)] (\mathbb{E}_{d \sim \tau(s)}[\phi(s, d)] - \sum_{s'} p(s' \mid s, a) \mathbb{E}_{d \sim \tau(s')}[\phi(s', d)])^T \\
&= \sum_s f(s) \sum_a \pi_{\mathbb{H}}(a \mid s) \frac{\varpi(a \mid s)}{\pi_{\mathbb{H}}(a \mid s)} \mathbb{E}_{d \sim \tau(s)}[\phi(s, d)] (\mathbb{E}_{d \sim \tau(s)}[\phi(s, d)] - \sum_{s'} p(s' \mid s, a) \mathbb{E}_{d \sim \tau(s')}[\phi(s', d)])^T \\
&= \sum_s f(s) \mathbb{E}_{d \sim \tau(s)}[\phi(s, d)] (\mathbb{E}_{d \sim \tau(s)}[\phi(s, d)] - \sum_a \varpi(a \mid s) \sum_{s'} p(s' \mid s, a) \mathbb{E}_{d \sim \tau(s')}[\phi(s', d)])^T \\
&= \Phi^T \mathbf{F}(\mathbf{I} - \mathbf{P})\Phi.
\end{aligned}$$

G Proof of Claim 1

We have that \mathbf{K} is positive definite if $\mathbf{S} = \mathbf{K} + \mathbf{K}^T$ is positive definite. Moreover, if \mathbf{S} is strictly diagonally dominant⁵, then it is also positive definite. Given that the diagonal elements of \mathbf{K} are positive and the off diagonal negative –see (i) below–, \mathbf{S} is strictly diagonally dominant if each row sum plus the corresponding column sum of \mathbf{K} is positive. This is because $S(i, j) = K(i, j) + K(j, i)$ if $i \neq j$ and $S(i, i) = 2K(i, i)$ so it must hold that:

$$\begin{aligned}
|S(i, i)| &> \sum_{i \neq j} |S(i, j)| \Rightarrow |2K(i, i)| > \sum_{i \neq j} |K(i, j) + K(j, i)| \\
&\Rightarrow |2K(i, i)| - \sum_{i \neq j} |K(i, j) + K(j, i)| > 0 \\
&\stackrel{(i)}{\Rightarrow} 2K(i, i) + \sum_{i \neq j} (K(i, j) + K(j, i)) > 0 \Rightarrow \sum_{i, j} K(i, j) + \sum_{i, j} K(j, i) > 0
\end{aligned}$$

This concludes the proof.

⁵The matrix \mathbf{A} is strictly diagonally dominant if $|a_{ii}| > \sum_{j, j \neq i} |a_{ij}|$ for every i

H Experiments: Additional Details

Here we provide additional details about the environment design and implementation of the methods.

H.1 Environment details

The sampling of each cell type during the environment generation depends on the traffic level of the corresponding row, following the distribution in Table 1. The traffic level of each row depends on the traffic level of the previous row according to the transition diagram in Figure 3. Each episode starts at a random row with traffic level `light`.

	road	grass	stone	car
no-car	0.7	0.2	0.1	0
low	0.6	0.2	0.1	0.1
heavy	0.5	0.2	0.1	0.2

Table 1: Cell type distribution

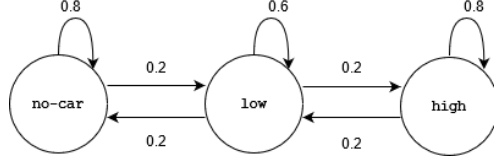


Figure 3: Traffic level transition diagram

H.2 Implementation details

We describe below the network architectures as well as the hyperparameters and some implementation specific choices we made in our experiments. For the development of the code we used Python 3.7 and PyTorch 1.8.1. In all experiments we used fixed random seeds for reproducibility. We note also that even though all algorithms ran once for each scenario— for time and computational reasons—, we observed consistency of the results across different scenarios.

Networks. The machine neural policy has the following representation: (a) the input is 76 binary features corresponding to the perceived state, (b) the output is the estimated log probability of each action, and (c) there is 1 hidden layer with 256 units and hyperbolic tangent activation. The option value function network has the following representation: (a) the input is 78 binary features (76 for the state and additional 2-bits encoding the agent in control), (b) the output is the estimated option value, and (c) there is 1 hidden layer same as for the machine neural policy.

Hyperparameters. To finalize the number of offline and online training episodes, we experimented with various combinations. For the offline stage we experimented with values in $[50, 100]$ with the incentive to achieve minimum cost without overfitting in all methods for all scenarios, for comparison reasons. For the online stage we chose per scenario from values in $\{50, 100, 200\}$ with the incentive to reach convergence, while saving computational time in all methods. We tried also different schedules for ϵ and chose the one resulting in optimal performance. In the offline stage, except the schedule applied in final experiments, we experimented also with: a) a fixed $\epsilon \in \{0.1, 0.2, 0.3\}$, b) $\epsilon = 0.3$ in the first half and $\epsilon = 0.2$ in the second half. In the online stage we assumed only decaying ϵ while trying different decay rates $1/t, 1/\sqrt{t}$. We used the selected schedule for ϵ in all scenarios in all methods. In all experiments we used RMSProp optimizer as used in the implementation⁶ of ACE [21] and COF-PAC [57] and empirically adjusted the initial learning rate to 10^{-4} after trying values in $\{10^{-3}, 10^{-4}, 10^{-5}\}$; our choice was based on stability and training efficiency. For simplicity of computation we used batch of size 1.

Implementation choices. In order to encourage exploration in the online stage we applied entropy regularization in the actor update with an initial weight of 0.01, decaying with rate $1/t$. Moreover, for this update in practice we used $c(s_t, a_t) + v_{\theta_t}^{\tau}(s_{t+1}) - v_{\theta_t}^{\tau}(s_t)$ to approximate the true $v^{\tau}(s_t)$ that is required in Eq. 12, as this increased the stability of our algorithm. To this end, in all experiments, we also used a

⁶<https://github.com/ShangtongZhang/DeepRL>

separate target network – a frozen copy of the option value function network, updated every 5000 steps– for the computation of $Q_{\theta_t}^{\tau}(s_{t+1}, d_{t+1})$ as in the implementation⁶.